Overview of TCV Results

A.Fasoli for the TCV Team[1]

Ecole Polytechnique Fédérale de Lausanne (EPFL)
Centre de Recherches en Physique des Plasmas
Association EURATOM-Confédération Suisse, CH-1015 Lausanne, Switzerland

E-mail contact of main author: ambrogio.fasoli@epfl.ch

Abstract. This overview highlights the progress accomplished on TCV during the 2004-2006 campaigns, along five main research avenues: particle, energy and momentum transport; edge physics; H-mode physics under strong electron heating; ECH and ECCD physics; scenarios with internal transport barriers and large non-inductive current fractions. Peaked density profiles are measured in the absence of a Ware pinch or a core particle source, demonstrating the essential role of anomalous processes. In terms of the influence of the plasma shape on energy confinement and transport, TCV data indicates that χ_e decreases significantly as the plasma triangularity is decreased. Measurements of the plasma toroidal rotation in the absence of external momentum input are inconsistent with diffusion of toroidal momentum from the edge. The comparison of SOL fluctuation measurements with the results of a fluid turbulence code indicates radial interchange motion of field-aligned plasma filaments as the cause of anomalous cross-field transport in the SOL. Third harmonic X3 heating (1.5MW) applied to ELMy H-modes leads to β~2.5% (β_N~2), large type I ELMs and peaked density profiles, significant ion heating (T_i up to ~1keV, with T_i/T_e~0.4), and to a transition to quasi-stationary ELM-free H-modes lasting for many energy confinement times. The supra-thermal electrons produced during strong EC heating and following sawtooth crashes are observed to undergo a very rapid cross-field transport. Electron Bernstein wave heating is demonstrated in the O-X-B conversion scheme, with a measurable increase in T_e and a deposition profile peaked where the density is beyond the O-mode cut-off. Electron internal transport barriers leading to significant confinement improvement (up to a factor of 6) compared to L-mode and bootstrap current fractions in excess of 70%, are obtained with strong ECCD in non-inductive scenarios, in cases with comparable ohmic and non-inductively driven currents, and, transiently, during current ramps in the absence of current drive. The key role of the current profile in the transition to improved confinement is demonstrated using small inductive current perturbations. A negative magnetic shear at the center is shown to be crucial for obtaining eITBs, whose strength increases for increasing shear. No special role of the rational q-surfaces in the barrier formation is observed.

1. Introduction

The *Tokamak à Configuration Variable*, TCV [1], addresses the scientific questions that have been recognised to limit our understanding of magnetically confined plasmas and our ability to control them in ITER relevant scenarios, and explores, at the same time, avenues for

[1] S. Alberti, P. Amorim (IST Lisbon, P), G. Arnoux, E. Asp, R. Behn, M. Bernard, P. Blanchard, A. Bortolon, A. Bottino, Y. Camenen, S. Coda, L. Curchod, B. Duval, E. Fable, A. Fasoli, W. Fundamenski (UKAEA, Cuhlam Science Center, UK), I. Furno, E.O. Garcia (Risö National Lab., DK), S. Gnesin, T. Goodman, J. Graves, A. Gudozhnik, B. Gulejova, M. Henderson, J.-Ph. Hogge, J. Horacek, B. Joye, A. Karpushov, I.Klimanov, H. Laqua (IPP-Greifswald, D) J.B. Lister, X. Llobet, T. Madeira (IST Lisbon, P), A. Marinoni, J. Marki, Y. Martin, M. Maslov, J.-M. Moret, A. Mueck, V. Naulin (Risö National Lab., DK), A.H. Nielsen (Risö National Lab., DK), I. Pavlov, V. Piffl (IPP Praha, CZ), R.A. Pitts, A. Pitzschke, A. Pochelon, L. Porte, J.J. Rasmussen (Risö National Lab., DK), O. Sauter, A. Scarabosio, H. Shidara, Ch. Schlatter, A.Sushkov (RRC Kurchatov, RF), G. Tonetti, M.Q. Tran, G. Turri, V. Udintsev, G. Véres (KFKI, Budapest, H), F. Volpe (IPP-Greifswald, D), H. Weisen, A. Zabolotskiy, A. Zuchkova, C. Zucca.

improving the plasma performance towards a conceptual fusion power plant that may not necessarily be investigated by an integrated experiment such as ITER [2]. The flexibility of the shaping and control systems, making TCV a unique research tool worldwide, is matched by that of its Electron Cyclotron Heating (ECH) and current drive (ECCD) systems. These include 3MW from six gyrotrons at 82.7GHz used at the second harmonic in X-mode (X2) [3], and 1.5MW from three gyrotrons at 118GHz (X3) [4].
This overview highlights the progress accomplished on TCV during the 2004-2006 campaigns, which were focussed on five general themes, reflected in the structure of the paper: Section 2 deals with particle [5], energy [6] and momentum transport in shaped plasmas, including recent findings on the spontaneous plasma rotation profile [7]; Section 3 discusses our recent efforts in plasma edge physics, mainly devoted to understanding the origin of anomalous cross-field transport in the SOL [8]; Section 4 addresses the physics of H-modes under strong electron heating at reactor relevant β [9]; Section 5 describes investigations on the physics of ECH and ECCD [9], including electron Bernstein waves [10]. These EC wave-plasma interactions can be used as tools to progress towards high performance, steady-state plasma scenarios, with electron internal transport barriers (eITBs) and large non-inductive current fractions [11], discussed in Section 6. A summary and an anticipation of possible future developments on TCV are included in Section 7, which concludes the paper.

2. Particle, Energy And Momentum Transport In Shaped Plasmas

The shape of the density profile is expected to have a significant impact on the performance of ITER and fusion reactors. Peaked profiles can increase the fusion power, but may also lead to a deleterious impurity accumulation in the reactor core. The behavior of particle and impurity density profiles is investigated in a number of different scenarios, including ECH and ECCD L-modes, eITBs and H-modes, with a view to improving our physics understanding and predictive capability for electron heated, ignited reactor conditions [5].
Fully ECCD sustained discharges in TCV show that density profiles can be peaked even in the absence of the Ware pinch [12]. Similarly, helium discharges, in which neutral penetration by successive charge exchange reactions is quenched because of the low cross section for double charge exchange, show that density profiles peak without a core particle source. In addition, neutral penetration calculations using the KN1D and DOUBLE-TCV codes confirm that the experimental density profiles are too peaked, even in deuterium plasmas, to be explained by edge fuelling and diffusive particle transport alone [13]. The combination of these observations provides the experimental proof that peaked density profiles may only be explained by anomalous processes.
Parametric scalings were obtained in L-mode, in which a wide range of operating conditions are easily achieved. The density peaking is found to scale with the peaking of the current profile and with the minor radius of ECH deposition for P_{ECH}>0.5MW.
The density profile is observed to flatten with additional core electron heating, but this effect saturates for a total power exceeding the ohmic power by more than a factor of three, as shown in Fig. 1. In contrast to L-modes, regimes characterised by reversed magnetic shear profiles and steady-state eITBs (see Section 6) do not show this profile flattening, even with central ECH. These results suggest that in a burning plasma, with strong core electron heating from fusion produced α's, the density profiles may remain peaked both with monotonic and reversed q-profiles, improving the fusion power output [14].
A concern for a reactor is that the large core electron heating by α's may destabilise TEMs, driving a thermo-diffusive outward particle flux, which may lead to partial or complete

flattening of the density profile [15]. This cannot be tested at JET yet, because purely ICRH heated H-modes in JET can only reach β_N~1 [16]. However, purely electron heated H-modes with $\beta_N \cong 2$ and $T_e/T_i \cong 2$, recently obtained in TCV using 1.5MW of ECH [9] (see Section 4), show only partial profile flattening and that significantly peaked profiles ($n_{e0}/\langle n_e \rangle$~1.5 in TCV ELMy H-modes) persist in electron heated regimes at reactor relevant values of β_N, even when T_e is significantly larger than T_i.

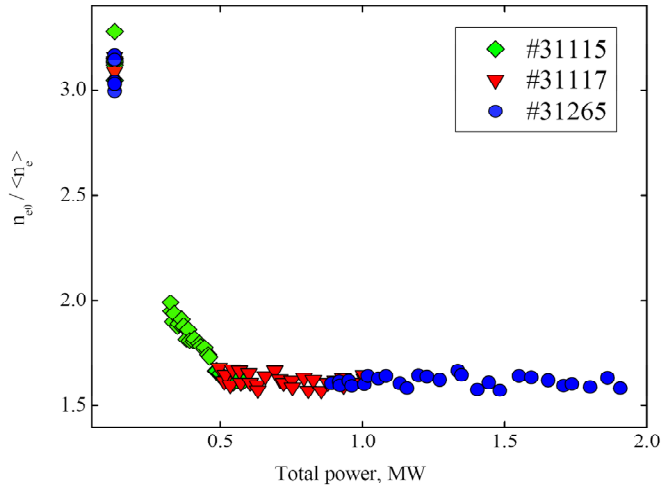

Fig. 1 *Density peaking as a function of the total power, indicating a clear saturation of flattening at high power. The plasma elongation, the minor radius and the toroidal magnetic field value are kept constant at κ=1.6, a=0.25m and B_T=1.44T.*

As the shape of the plasma cross-section influences a number of important plasma properties, experiments that can vary the plasma shape in a controlled way over a large range can lead to a better understanding of the physics determining these properties and, in practice, to identifying ways to control them. In particular, the influence of the plasma shape on the core energy confinement and electron heat transport was investigated in TCV plasmas over a wide range of plasma collisionalities, ν_{eff} (~0.15-2), including low density EC heated plasmas, with localized EC deposition just outside the q=1 surface, at normalised radius ρ=0.4 [17]. The effective collisionality is defined as the electron-ion collision frequency normalised to the electron curvature drift frequency, $\nu_{eff}=\nu_{ei}/\omega_{De}$, and has a simple dependence on plasma parameters, $\nu_{eff} \sim R_0 n_e Z_{eff}/T_e^2$. This study is restricted to L-mode conditions, with a plasma configuration limited on the central column, to avoid a strong influence of the plasma edge stability and parameters on the results.

Practically no plasma current is driven by the EC system, as the injection geometry is adjusted to be perpendicular to the field line at each plasma triangularity. The electron heat transport is quantified experimentally via the electron heat diffusivity, χ_e, defined from a power balance relation, in which the heat flux accounts for the contributions of the EC heating, the ohmic, and the electron-ion equipartition power, quoted in order of importance.

Fig. 2 shows that for the large values of normalised temperature gradient characteristic of these experiments (R/L_{Te}>10), χ_e decreases significantly for increasing plasma collisionality for each plasma shape, and as the plasma triangularity is decreased (δ from +0.4 to -0.4). The measured scaling of χ_e with T_e, density and effective charge is compatible with χ_e depending on these parameters only through ν_{eff}.

No significant MHD activity is detected in these discharges and the sawtooth activity is observed to have only a minor effect on the pressure profile around mid-radius, where the experimental points are taken. In addition, the variations of the safety factor profile with triangularity are only minor, and are not observed to influence χ_e.

On the other hand, an important role of TEM in electron heat transport is suggested by linear gyro-fluid [18] and gyro-kinetic models [19], which predict TEM to be the most unstable modes in these plasmas, and that their stability depends on ν_{eff} and δ in a similar way as the measured electron heat transport.

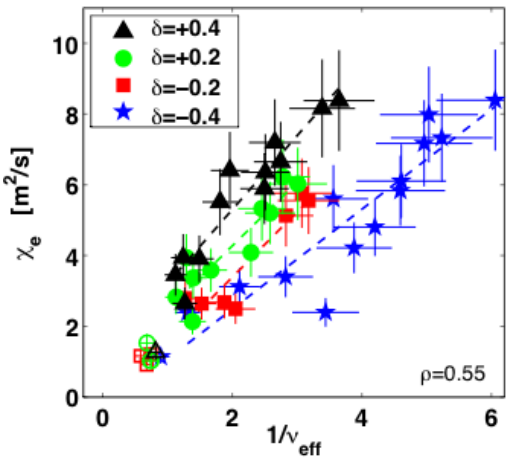

Fig. 2 *Experimental electron heat diffusivity at mid-radius as a function of plasma effective collisionality at four different values of plasma triangularity. Full symbols refer to EC-heated L-mode plasmas, while open symbols indicate ohmic plasmas, in which electron transport seems unaffected by plasma triangularity.*

The question of plasma rotation in toroidal devices is receiving increasing attention due to its impact on the stability of resistive wall modes, neoclassical tearing modes and micro-instabilities causing anomalous transport [20]. TCV can provide unique insight into the mechanisms generating and regulating plasma rotation, and the related interplay between particle, energy and momentum transport, using its ohmic and electron heated discharges with minimum external momentum injection. These investigations benefit from the diagnostic Neutral Beam, which directly induces a very small rotation (~1 km/s, compared to ~20 km/s in other machines), due to a combination of quasi orthogonal injection angle, and a modest average deposited power (20 kW).

Stationary toroidal rotation profiles are studied in steady-state ohmic L-mode discharges as a function of plasma current and electron density. For plasma currents I_p<380kA and central densities n_{e0} up to $8\times10^{19}m^{-3}$ the plasma is found to rotate in the counter current direction (the electron diamagnetic drift direction), with absolute values of the angular frequency $\omega_\phi=v_\phi/R$ up to 40krad/s at the plasma center, decreasing towards zero at the edge [21]. The rotation profile is flat or hollow inside the sawtooth inversion radius (Fig. 3a), whereas at low I_p, when the q=1 surface is absent, simply increases in magnitude from the edge to the center (not shown). As observed in other tokamaks, the toroidal rotation profile is strongly linked to the ion transport. Outside the inversion radius, the stationary rotation profile follows the T_i profile. Measurements of rotation profiles for both positive and negative current stationary discharges can be cast into an empirical scaling law [21] $v_{\phi,Max}$ [km/s] = $-12.5T_i/I_p$ [eV/kA], linking the maximum toroidal velocity along the profile to the ion temperature on axis and the plasma current (Fig 3b). In contrast to the NBI heated discharges, no direct dependence on the plasma density is measured.

A different regime is observed in high density ($n_{e0}>6\times10^{19}$ m^{-3}), high current (I_p>270 kA) plasmas, with the central toroidal rotation directed with the plasma current (the ion diamagnetic drift direction) [7]. Experiments with controlled density ramps demonstrate that, for a given plasma current, the transition to this regime occurs at a fixed central density value, $n_{e0}\sim6\times10^{19}$ m^{-3} (Fig. 4).

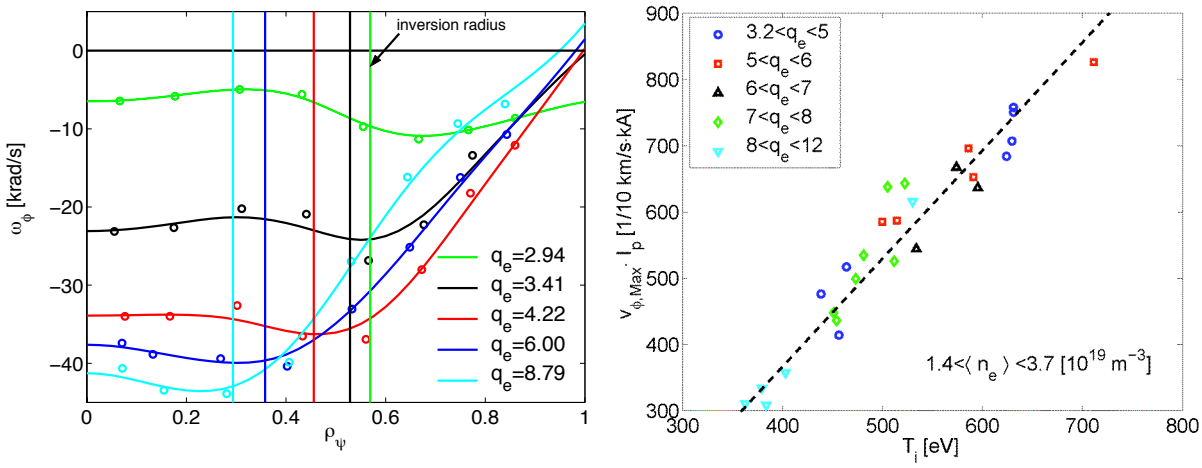

***Fig. 3 Left**: Angular velocity for different edge safety factors in positive plasma current discharges. Circles represent the experimental measurements. Vertical lines indicate the sawtooth inversion radius obtained from the tomography inversion of the soft X-ray emissivity. **Right**: Dependence of the maximum toroidal velocity weighted by the plasma current, $v_{\phi,max} \cdot I_p$, on the central ion temperature. The database encompasses positive and negative plasma currents.*

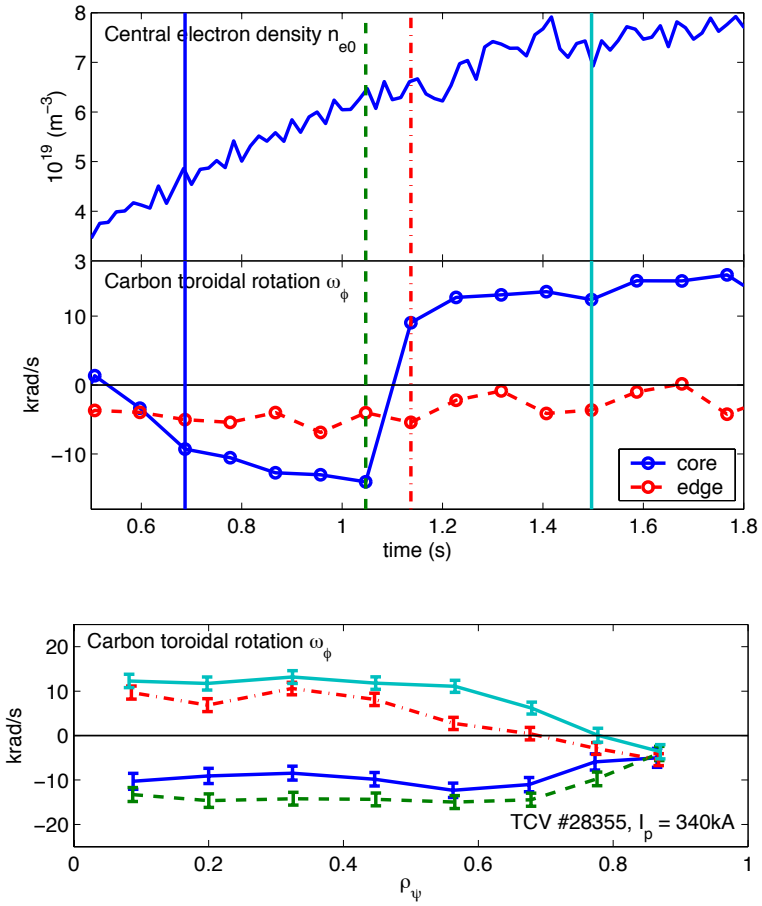

***Fig. 4** Transition form counter to co-current rotation regime during a density ramp in a limited L-mode discharge (I_p=340kA).*

After the transition, the rotation is positive inside ρ=0.7, with absolute values comparable with those before the transition. The rotation at the edge (ρ>0.8) remains unaffected. Intermediate rotation profiles show that the central part of the plasma appears to accelerate

rigidly in the co-current direction. These observations are not consistent with diffusion of toroidal momentum from the edge region, suggesting instead a change in the balance of internally generated sources of momentum.

3. Plasma Edge Physics

Anomalous cross-field transport of particles and energy is also a characteristic of the tokamak Scrape-Off-Layer (SOL). Its study is a major component of the TCV edge physics program [8]. Probe measurements in the SOL of TCV L-mode plasmas reveal that as the line-averaged core density increases, the particle density profile in the far SOL becomes broader in both radial extent and length scale. The plasma density increases throughout the SOL, which leads to recycling on the main chamber walls. In the region where the profiles are broad, the magnitude and radial variation of the fluctuation statistics of particle density and flux appear to be invariant with respect to changes in the core line average density.
Using the turbulent radial flux estimated from the data as a means to derive an effective diffusivity (via the commonly employed flux-gradient paradigm) yields values that vary significantly both with plasma density and radial distance in the SOL. As a consequence, no simple parameterisation of the turbulent particle flux in terms of diffusivity alone can be found for these TCV plasmas. Instead, an effective convection velocity provides a more stable description of transport, particularly at higher density in the main SOL. This is consistent with the radial motion of plasma filaments being the origin of intermittent SOL transport.
At the wall radius, the TCV data shows a linear dependence of the local turbulent particle flux on the local particle density, and a scaling that is close to quadratic with the line average density, as shown in Fig. 5. The implication is that the plasma flux at the wall intersection point can adequately be described only in terms of an effective convection velocity. A similar scaling for the particle outflux has been reported from other tokamaks [22] but these TCV measurements unambiguously identify cross-field turbulent transport as the origin.

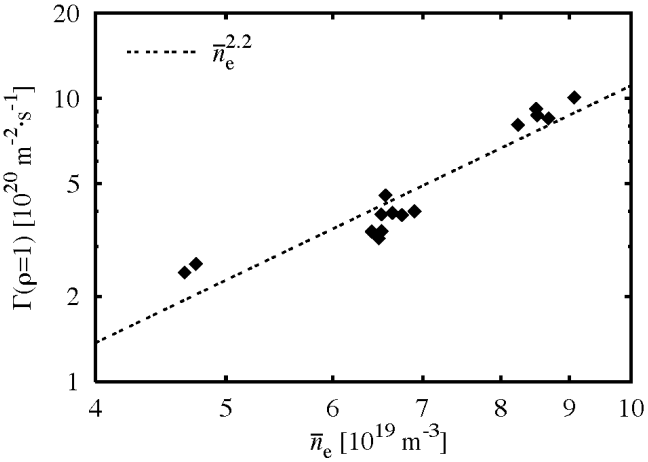

Fig. 5 *Variation of the turbulence driven particle flux density at the wall radius with the line-averaged density. The dotted line indicates a fitted power law function, which gives an exponent of 2.2.*

Mach probe measurements in the SOL reveal a significant parallel flow component that is independent of the toroidal field direction and is directed away from the outer mid-plane. The magnitude and direction of this *offset* flow component are consistent with estimates of a parallel flow driven by turbulent radial plasma and heat transport in the SOL. The measured magnitude and radial variation of statistical moments, temporal correlations, and the estimated transport-driven parallel flows are well reproduced by 2D fluid turbulence simulations using the ESEL code [23]. This provides convincing evidence that turbulent

transport, main chamber recycling, and the field independent parallel flow offset observed in tokamak experiments are due to rapid (100-200m/s) radial interchange motions of field-aligned plasma filaments in the SOL.

4. H-Mode Physics Under Strong Electron Heating At Reactor Relevant β

To further assess the potential of different plasma shapes in terms of plasma performance and more specifically β limits, a third harmonic EC heating system, with power up to 1.5MW, is employed on TCV [4]. Higher density plasmas than with the second harmonic system can be heated, in which a higher ion temperature is obtained from electron-ion collisional energy transfer [24]. Third harmonic X3 heating is applied to target plasmas in the ELMy H-mode, which exhibit relatively high energy confinement (τ~45ms) and temperatures (T_e~1keV, T_i~550eV), contributing to initiate the X3 absorption, which then progressively improves as the temperature rises [9]. Such targets, in single-null divertor configuration with the ion diamagnetic drift direction away from the X-point, have good vertical stability and densities close to optimal for X3 absorption, corresponding to about 25% of the Greenwald limit.
In these conditions, full power X3 heating raises the plasma β up to 2.5% (β_N~2), with large type I ELMs. Central electron and ion temperatures increase to ~2.5keV and ~1keV, respectively, corresponding to the most significant ion heating observed on TCV. At the same time, despite the absence of momentum input, a clear increase in the carbon ion toroidal rotation is detected. At high β the plasma is observed to undergo a transition to a quasi-stationary ELM-free H-mode, lasting for many energy confinement times, with the same density as ELMy discharges and significantly lower particle confinement than transient ELM-free H-modes.

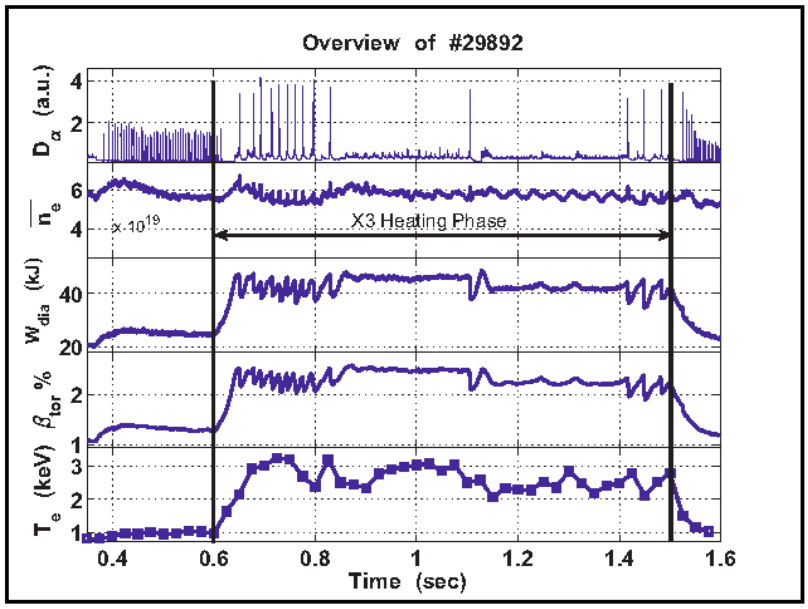

Fig. 6 *Overview of a TCV discharge (29892) exhibiting a transition to a quasi-stationary ELM-free H-mode. From top to bottom: D_α-light, line average density, stored energy, β_{tor} and electron temperature. The ELMy H-mode target is heated using 1.4MW of X3 power.*

This regime is characterised by D_α-light emission stronger than in the Type III ELMy H-mode, approximately constant electron density, diamagnetic energy and toroidal β (β_{tor}~2.5%, while the ideal limit is at 3.5%). The confinement corresponds to an H-mode enhancement factor in the range $H_{IPB(y,2)}$~1.4-1.7. Fig. 6 shows an example of such discharge. Measurements

of soft X-ray emission reveal no sign of impurity accumulation during the quasi-stationary ELM-free phase. The effective charge is $Z_{eff} \approx 2.5$ in the ohmic phase and increases to ≈ 3 in the X3 phase. This quasi-stationary ELM-free H-mode reaches reactor relevant normalised β ($\beta_N \sim 2$) without direct ion heating, active fuelling or cryo-pumping.

5. ECH And ECCD Physics, Including Electron Bernstein Waves

The dynamics of supra-thermal electron is investigated thoroughly in TCV, as it is intrinsically related to the efficiency of the main heating and current drive systems, based on EC wave-particle interactions [25, 9]. A distinct supra-thermal electron population is observed not only during strong EC heating, but also following sawtooth crashes. Different ECH-ECCD scenarios, including X3 vertical injection, are used to manipulate the electron distribution and study its dynamics. Low duty cycle EC bursts and coherent averaging of the relevant signals provide information on EC wave induced diffusion of fast electrons, their collisional slowing-down and pitch angle scattering in velocity space, as well as on their real space transport [26].
High field side measurements of the ECE emission, interpreted assuming a simple bi-Maxwellian electron distribution, and that the relatively tenuous supra-thermal component is optically thin, provide the supra-thermal density profile. The broadening of the profile due to radial transport, and the decay in time, due to collisional momentum scattering, are clearly distinguished. By applying a simple diffusive model, a supra-thermal diffusion coefficient and a typical decay time are extracted from the data, as shown in Fig. 7. Very fast diffusion ($D > 10$ m^2/s) is generally found [26], although more complete (Fokker-Planck) modelling of the phase space transport of the supra-thermal component is needed to fully unfold the system dynamics. Nevertheless, electrons accelerated by electric fields associated with the magnetic reconnection occurring at sawtooth crashes are also observed to undergo a very rapid cross-field transport, with $D > 20$ m^2/s [27].

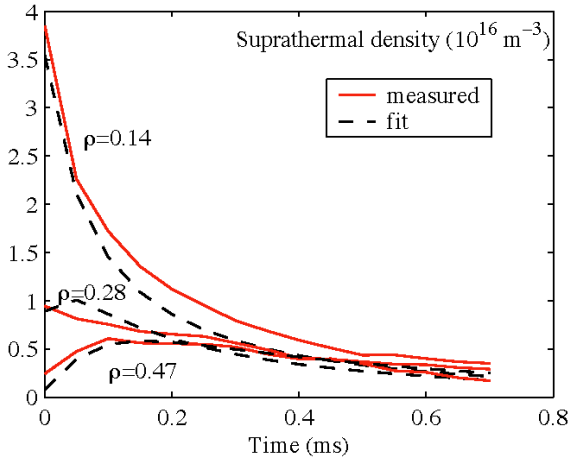

Fig. 7 *Measured and fitted time traces of the supra-thermal density at three different radial locations, for the case of Fig. 5. The fit is based on a cylindrical diffusive model with diffusivity D=12.6 m^2/s and decay time of 1.5 ms. The average injected power is 40 kW, the plasma current 230 kA and the line averaged density 1.5x10^{19} m^{-3}.*

Heating plasmas at densities above the second harmonic X-mode cut-off can lead to increasing both the plasma confinement and the pressure. The means to achieve high-density electron heating on TCV include quasi-vertically launched X3 ECH, discussed in Section 4, and low field side injected Electron Bernstein wave heating (EBH) [28, 10]. EB waves are not subject to X2 cut-off, hence can be used to circumvent the limitation to the plasma density

that can be accessed by O- and X-mode EC. The O-X-B scheme is used on TCV, where the large densities and density gradients necessary for the O-X conversion are obtained in diverted H-modes with specific values of triangularity and edge safety factor, δ~0.55 and q_{95}~2.5 [10]. The optimum injection angle for the O-X-B conversion is determined experimentally by varying the injection angle of EC waves modulated at a low duty cycle (6%) and measuring the microwave stray radiation. The measured value of the optimum angle is in very good agreement with the predictions of the ART ray tracing and double mode conversion code [29].

EC waves modulated with a higher duty cycle (46%) are injected to measure the global and local EBH power deposition. An average absorbed power fraction of about 60% is measured from diamagnetic measurements for densities well above the cut-off. The spatial distribution of the power absorption is determined experimentally from a Fourier analysis of the soft X-ray emissivity. The deposition radius is observed to be well inside the plasma cut-off and to match the value predicted by ART to within the experimental uncertainties (Fig. 8). Note that these modulated power deposition measurements are performed with a relatively far off-axis deposition (ρ=0.7), to avoid strong sawtooth perturbations.

To demonstrate EBH over periods longer than the confinement time, long pulses and a more central power deposition scheme (ρ=0.4) are used. A central temperature increase of up to 80eV is measured consistently by Thomson scattering and the soft X-ray absorber method [10]. These results constitute the first demonstration of heating by O-X-B double mode conversion in an overdense, conventional aspect-ratio tokamak and motivate further investigations of the potential of using EBH or EBCD in H-modes of large tokamak devices.

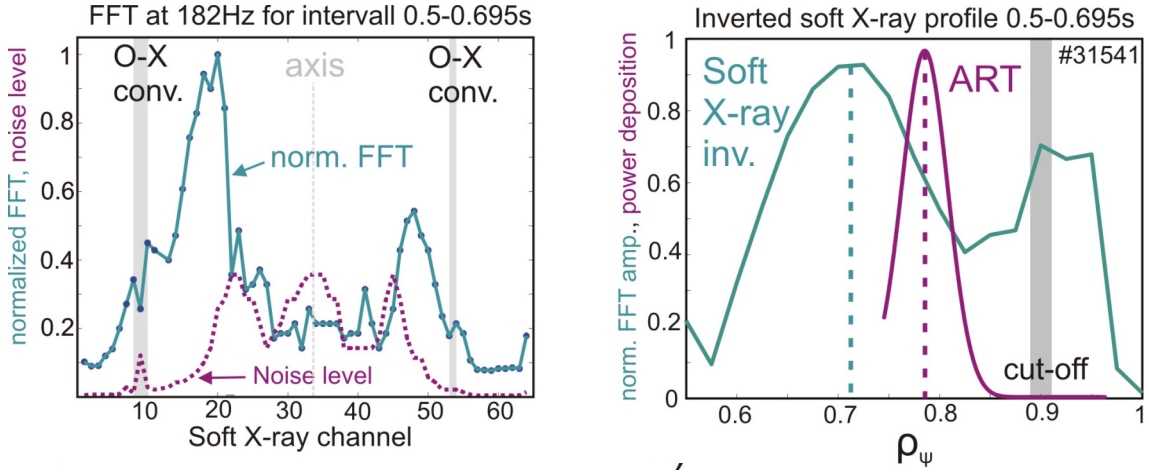

***Fig. 8 Left**: Profile of the normalized FFT amplitude of the line-integrated soft X-ray time traces at the modulation frequency of the injected EC waves at 182 Hz (green). The noise level, due to sawteeth, is shown for reference (violet). **Right**: Local soft X-ray emissivity oscillation amplitudes at the modulation frequency, derived by inverting the line-integrated soft X-ray chords signals (green). The resulting deposition profile (peaked at ρ~0.71) is compared with that of the deposited beam power calculated by the ART code (peaked at ρ~0.78). The residual power deposited outside the cut-off, visible in the edge soft X-ray signals, is presumably due to 2nd harmonic X-mode absorption of non-converted wave power subject to multiple wall reflections.*

6. Physics Of Improved Steady-State Tokamak Regimes

Electron Internal Transport Barriers (eITBs) are obtained on TCV in a variety of experimental conditions [11], with strong ECCD in nearly or fully non-inductive scenarios [30-31], in cases with comparable ohmic and non-inductively driven currents [32], and, transiently, by strong

heating during current ramps [11]. Fully non-inductive scenarios involve an appropriate distribution of ECCD sources to sustain a hollow current profile, further enhanced by the bootstrap current centered in the high gradient barrier region [33]. Depending on the details of the discharge parameters and conditions, these scenarios may evolve to steady-state, lasting several current redistribution times and up to hundreds of electron energy confinement times. A significant (up to a factor of 6) improvement in confinement compared to TCV L-mode scaling and strongly correlated barriers in n_e and T_e characterize all these conditions. The highest performance discharges also display high bootstrap current fractions and high poloidal β. Higher enhancement factors are obtained in non-stationary conditions, and the bootstrap fraction reaches 90% transiently during early current ramps.
Recent experiments, in which small current perturbations are produced inductively with negligible energy input, confirm the key role of the current profile in the transition to improved confinement. Small increases or decreases in the central current density can dramatically degrade or enhance the confinement, respectively, while the location of the barrier is largely unaffected (Fig. 9) [30]. This experiment replicates in a more controlled fashion the results of earlier studies performed with varying central ECCD components [32] and confirms that a negative central magnetic shear is crucial to the creation of a barrier. The strength of the barrier is observed to increase with the magnitude of the shear.

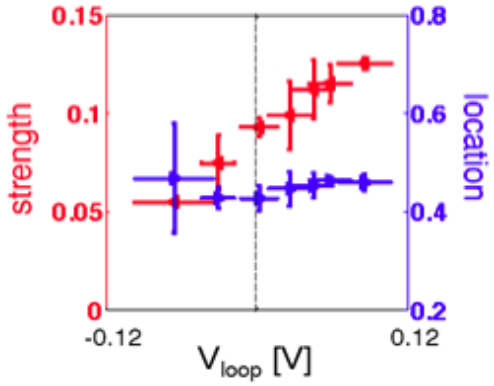

Fig. 9 *Electron internal transport barrier strength (quantified by the ion sound gyro-radius normalized to the electron temperature gradient scale length on the outer mid-plane) and location (radial coordinate equal to the normalised square root of the plasma volume) as functions of the surface loop voltage for a set of ohmic current perturbation experiments in otherwise non-inductive discharges.*

In apparent contrast to other experiments, no special role appears to be played on TCV by rational q-surfaces in the electron barrier formation (in the range $1.3<q<2.3$), as suggested by the observed smooth dependence of the confinement enhancement on the applied perturbative loop voltage (see Fig. 10). The eITBs are also characterised by sizeable density gradients, with $\nabla n/n \sim 0.5 \nabla T_e/T_e$, sustained by an inward pinch of thermo-diffusive nature [34].
Both in non-inductive and inductive eITB scenarios, slow oscillations of the electron temperature, with frequency ~10Hz and full poloidal and toroidal symmetry (m=n=0), are observed, coexisting with MHD modes [11]. This phenomenon appears akin to the O-regime on the Tore Supra tokamak, occurring in fully or nearly non-inductive discharges with lower hybrid current drive and negative central magnetic shear [35]. The oscillations affect the whole plasma column, as the total plasma current oscillates (with a 45° phase shift with respect to the temperature oscillations) and the magnetic axis shifts radially by up to 3 cm. A feedback mechanism therefore appears to be at play, in which the MHD mode degrades the confinement, which in turn reduces the gradients and the MHD instability drive, so that a regular oscillatory pattern is established.

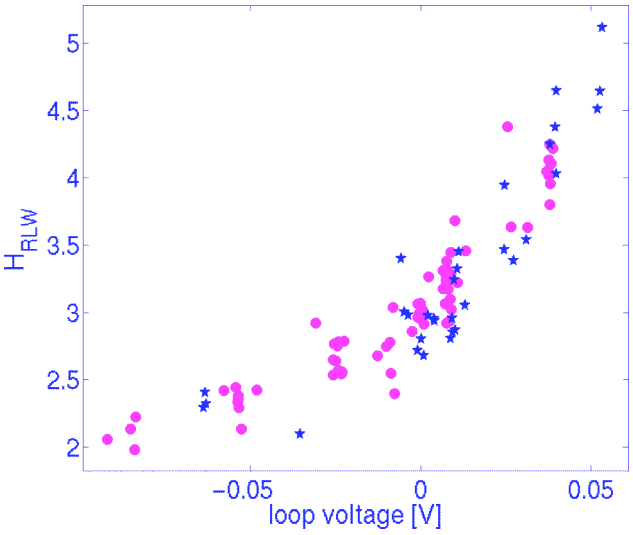

Fig. 10 *Confinement-enhancement factor in the steady-state phase vs. loop voltage applied to an established eITB (blue) or before the barrier formation (magenta). A negative voltage corresponds to a positive current. Both 1.35MW (stars) and 2.25MW (circles) ECCD data is shown.*

7. Summary and Outlook

The results obtained on TCV during the past few years contribute to demonstrating important properties of regimes of interest for ITER and future experimental reactors and to improving the basic understanding of the underlying physics.

Peaked density profiles are measured in the absence of a Ware pinch or a core particle source, demonstrating the essential role of anomalous processes. The density profile flattening observed with additional core electron heating saturates at large power values, suggesting that in a burning plasma, with strong core electron heating from fusion produced α's, the density profiles may remain peaked, improving the fusion power output.

In terms of the influence of the plasma shape on energy confinement and electron heat diffusivity, TCV data indicates that at low collisionalities χ_e decreases significantly as the plasma triangularity is decreased and that the measured scaling of χ_e with other plasma parameters can be cast into a dependence only upon ν_{eff}. Measurements of the plasma toroidal rotation profile and its dynamical evolution in the absence of external momentum input cannot be interpreted on the basis of diffusion of toroidal momentum from the edge. The comparison of fluctuation measurements in the plasma SOL with the results of a fluid turbulence code indicates that anomalous cross-field transport in the SOL originates from rapid radial interchange motions of field-aligned plasma filaments.

Third harmonic X3 heating (1.5MW) applied to ELMy H-modes leads to plasma β up to 2.5% (β_N~2) with large type I ELMs and peaked density profiles, to significant ion heating (T_i up to ~1keV, and $T_i/T_e \geq 0.4$), and to a transition to a quasi-stationary ELM-free H-mode lasting for many energy confinement times. The supra-thermal electron population produced during strong EC heating and following sawtooth crashes is observed to undergo a very rapid cross-field transport.

The limitation to the plasma density accessible by O- and X-mode EC waves can be circumvented by using Electron Bernstein waves. In the O-X-B scheme, T_e increases of ~10% are measured, with power absorption fractions up to 60% and a deposition profile peaked where the density exceeds the O-mode cut-off value, clear signatures of EBW heating.

Electron internal transport barriers leading to significant confinement improvement (up to a factor of 6) compared to L-mode, with bootstrap current fractions in excess of 70%, are obtained on TCV with strong ECCD in non-inductive scenarios, in cases with comparable ohmic and non-inductively driven currents, and, transiently, in the absence of current drive during current ramps. The key role of the current profile in the transition to improved confinement is demonstrated using small current perturbations produced inductively. A negative magnetic shear at the center is shown to be crucial for obtaining eITBs, whose strength increases with increasing reverse shear, while no evidence for a special role of the rational q-surfaces in the barrier formation is found.

In the future, closer comparisons with theoretical predictions, including nonlinear kinetic models unavailable until recently, are expected to further our understanding of anomalous heat and particle transport. To this end, diagnostics upgrades are anticipated on TCV, particularly to measure the current profile, using polarimetry, and to estimate poloidal rotation and radial electric fields. The recent edge density fluctuation measurements constitute the first step towards a complete characterisation of turbulent transport and density and temperature fluctuations at different poloidal locations, including far away from the ballooning region. Comparisons between SOL flow measurements and core and edge rotation data from CXRS can help elucidate the role of SOL flows in generating toroidal rotation in the absence of direct momentum input, a fundamental question for ITER and reactor plasmas. A new digital control system will be installed to optimise X3 absorption and the control of MHD instabilities and pressure and current profiles using EC waves. Part of the TCV campaigns will be dedicated to questions related to the access and the control of steady-state scenarios with internal transport barriers, in particular with large bootstrap current fractions. Future experiments will extend the eITBs to higher performance using the full ECH system, achieve 100% bootstrap current fraction, control the barrier formation, study any hysteresis properties of the barrier formation, and test the transport of energy, particles and impurities across and inside the barrier location.

More generally, an important element for adding to the fusion relevance of the medium term TCV scientific program is the attainment of plasma regimes with comparable electron and ion temperatures, and with high β values. These two goals are interrelated. An enhanced ion-electron collisional coupling can be achieved in relatively high-density plasmas, and high β requires operation at high current and high elongation. Both conditions require plasma densities above the X2 cut-off. The X3 ECH system has already extended the range of densities achievable on TCV, increasing the plasma β. The Electron Bernstein wave heating experiments at 83GHz are exploring the potential of such auxiliary heating method, not subject to density cut-off. In addition, two longer term options for TCV are under consideration, the installation of auxiliary ion heating, and the operation at higher field, allowing us to use the 118 GHz system at the second harmonic, but with an increased value of the density cut-off. Operating at higher plasma densities and T_i/T_e ratios will allow TCV to further address transport, confinement, MHD limits, LH transitions and possibly ELM and NTM mitigation and control methods in a critical part of the tokamak operational space and with a range of plasma shapes that are inaccessible to other devices.

This work was partly supported by the Fonds National Suisse pour la Recherche Scientifique.

References

[1] HOFMANN, F. et al., Plasma Phys. Control. Fusion 36 (1994) B277.
[2] ITER Physics Basis Editors et al., Nucl. Fusion 39 (1999) 2137.
[3] GOODMAN, T.P. et al., Proc. of 19th Symp. on Fusion Technology, Vol.1, p.565, Lisbon (1996).
[4] HOGGE, J.P. et al., Nucl. Fusion 49 (2003) 1353.

[5] ZABOLOTSKY, A. et al., Paper EX/P3-7, this Conference.
[6] CAMENEN, Y. et al., Paper EX/P3-20, this Conference.
[7] BORTOLON, A. et al., to be published on Phys. Rev. Lett. (2006).
[8] HORACEK, J. et al., Paper EX/P4-21, this Conference.
[9] PORTE, L. et al., Paper EX/P6-20, this Conference.
[10] POCHELON, A. et al., Paper EX/P6-2, this Conference.
[11] CODA, S. et al., Paper EX/P1-11, this Conference.
[12] ZABOLOTSKY, A. et al., Plasma Phys. Control. Fusion 45 (2003) 735.
[13] ZABOLOTSKY, A. et al., Nucl. Fusion 46 (2006) 594.
[14] ZABOLOTSKY, A. et al., Plasma Phys. Control. Fusion 48 (2006) 369.
[15] GARBET, X. et al, Plasma Phys. Control. Fusion 46 (2004) B577.
[16] WEISEN, H. et al, Paper EX/8-4, this Conference.
[17] CAMENEN, Y. et al., Plasma Phys. Control. Fusion 47 (2005) 1971.
[18] WALTZ, R.E. et al., Phys. Plasmas 4 (1997) 2482.
[19] BOTTINO, A. et al., Phys. Plasmas 11 (2004) 198.
[20] RICE, J.E. et al. Physics of Plasmas, 11 (2004) 2427.
[21] SCARABOSIO, A et al, Plasma Phys. Control. Fusion 48 (2006) 63.
[22] LABOMBARD, B. et al., Paper EX5/6, 18th IAEA Fusion Energy Conference, Sorrento, Italy, (2000).
[23] GARCIA, O.E., Phys. Rev. Lett. 92 (2004) 165003.
[24] ALBERTI, S. et al., Nucl. Fusion 45 (2005) 1224.
[25] CODA, S. et al., Nucl. Fusion 43 (2003) 1361.
[26] CODA, S. et al., to be published on Plasma Phys. Control. Fusion (2006).
[27] KLIMANOV, I., Ph.D. Thesis no. 3432, Ecole Polytechnique Fédérale de Lausanne (2005).
[28] BERNSTEIN, I., Phys. Rev. Lett. 109 (1958) 10.
[29] VOLPE, F. and LAQUA, H.P., Rev. Sci. Instrum. 74 (2003)1409.
[30] SAUTER, O. et al, Phys. Rev. Lett. 94 (2005) 105002.
[31] HENDERSON, M.A. et al., Phys. Rev. Lett. 93(2004) 215001.
[32] HENDERSON, M.A. et al., Plasma Phys. Control. Fusion 46 (2004) A275.
[33] GOODMAN, T.P. et al., Plasma Phys. Control. Fusion 47(2005) B107.
[34] FABLE, E. et al., Plasma Phys. Control. Fusion 48 (2006) 1271.
[35] GIRUZZI, G. et al., Phys. Rev. Lett. 91 (2003) 135001.